Chemosphere 350 (2024) 140950

Contents lists available at ScienceDirect

Chemosphere

journal homepage: www.elsevier.com/locate/chemosphere

Effects of gadolinium (Gd) and a Gd-based contrast agent (GBCA) on early life stages of zebrafish (*Danio rerio*)

Stefania Piarulli [a,*,1], Juliane A. Riedel [b,1], Frida N. Fossum [c], Florence Kermen [c,d], Bjørn Henrik Hansen [a], Bjarne Kvæstad [e], Pål A. Olsvik [b], Julia Farkas [a,**]

[a] Department of Climate and Environment, SINTEF Ocean, Brattørkaia 17C, 7010, Trondheim, Norway
[b] Faculty of Biosciences and Aquaculture, Nord University, Universitetsalléen 11, 8026, Bodø, Norway
[c] Department of Biology, Norwegian University of Science and Technology, Høgskoleringen 5, 7491, Trondheim, Norway
[d] Department of Neuroscience, University of Copenhagen, Blegdamsvej 3b, 2200, Copenhagen, Denmark
[e] Department of Fisheries and New Biomarine Industry, SINTEF Ocean, Brattørkaia 17C, 7010, Trondheim, Norway

HIGHLIGHTS

- Two forms of gadolinium (Gd) were tested for acute toxicity and sublethal effects.
- Embryos were exposed for 96 h to 3–3000 μg Gd L^{-1}.
- None of the two tested compounds were acutely toxic.
- No effects on larvae development and locomotive behaviour were observed.
- The highest exposure concentrations affected the larvae's brain activity.

GRAPHICAL ABSTRACT

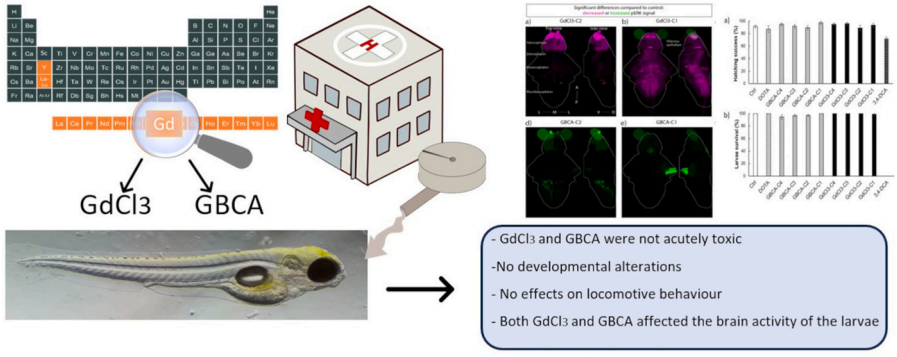

ARTICLE INFO

Handling editor: James Lazorchak

Keywords:
Rare earth elements
REE
Ecotoxicity
Embryotoxicity
Neurotoxicity
Fish

ABSTRACT

Gadolinium (Gd) is one of the rare earth elements (REY) and is widely used in magnetic resonance imaging (MRI) contrast agents. Anthropogenic Gd enrichment has frequently been found in wastewater treatment plant effluents in industrialised countries, rising concerns regarding effects on aquatic biota. This study investigates the acute toxicity and sublethal effects of Gd in two forms, as inorganic salt ($GdCl_3$) and as Gd-based contrast agent (GBCA), on early life stages of zebrafish (*Danio rerio*). Nominal exposure concentrations ranged from 3 to 3000 μg L^{-1}, with an exposure duration of 96 h. None of the two tested compounds were acutely toxic to embryos and larvae. Similarly, we did not observe any effects on larval development and locomotive behaviour. However, we found significant changes in the brain activity of larvae exposed to the highest concentrations of $GdCl_3$ and the GBCA. Our findings show that Gd can have sublethal effects on developing fish at lower concentrations than

* Corresponding author.
** Corresponding author.
E-mail addresses: stefania.piarulli@sintef.no (S. Piarulli), julia.farkas@sintef.no (J. Farkas).
[1] The authors contributed equally to this work.

https://doi.org/10.1016/j.chemosphere.2023.140950
Received 18 November 2023; Received in revised form 5 December 2023; Accepted 11 December 2023
Available online 17 December 2023

reported previously, highlighting the necessity of investigating the long-term fate and effects of GBCAs released into the aquatic environment.

1. Introduction

The 15 rare earth elements plusyttrium (REY) are a geochemically coherent and relatively homogeneous group of elements that are widely distributed in the Earth's crust (Kamenopoulos et al., 2015). Their unique (electro)chemical properties make REY technology-critical elements, being important in a wider range of industrial applications throughout the last decades (Gwenzi et al., 2018). Increasing emissions of REY can cause anomalous enrichment in aquatic environments, where they can persist, can be transported in different compartments and have the potential to cause ecotoxicological effects (for review see Piarulli et al., 2021).

Gadolinium (Gd) is one of the anthropogenically most utilized REY and is applied in metallurgy, magneto-optics and nuclear marine propulsion (Gwenzi et al., 2018). It is also a particularly important component of contrast agents used for magnetic resonance imaging (MRI), with around 50 metric tonnes administered annually worldwide (Wahsner et al., 2019). Due to the known toxic properties of free Gd ions (Gd^{3+}) to humans, Gd-based contrast agents (GBCAs) are designed as inert chelate complexes that undergo no metabolization in the human body (Caravan et al., 1999). However, it has recently been shown that Gd^{3+} can dissociate spontaneously from its ligand depending on the specific properties of the latter, such as polarity and linearity (Port et al., 2008). While spontaneous dissociation occurs rather rarely under physiological pH, transmetalation, the replacement of Gd^{3+} by endogenous competing ions such as calcium (Ca^{2+}) and Zinc (Zn^{2+}), has been identified as a common process for Gd-chelates (Runge, 2018). Wastewater treatment plants (WWTP) collecting hospital effluents represent a major source for GBCAs, which can pass conventional treatment systems largely unaffected (Kümmerer and Helmers, 2000). It has been shown that anthropogenic Gd can reach several μg L^{-1} in wastewater receiving waters (Bau and Dulski, 1996; Brünjes and Hofmann, 2020; Knappe et al., 2005; Merschel et al., 2017; Parant et al., 2018), while naturally, rivers show geogenic background levels in the low ng L^{-1} range (Bau and Dulski, 1996; Kümmerer and Helmers, 2000).

GBCAs, compared to free Gd, generally have a higher chemical stability and can remain dissolved in the aqueous phase for extended time (Bau and Dulski, 1996), therefore, having a great potential for longer-range transport in aquatic systems and bioavailability for pelagic organisms (Hatje et al., 2016; Nozaki et al., 2000). Albeit their widespread occurrence, bioavailability and potential for bioaccumulation, there is a substantial lack of comprehensive information regarding GBCA and Gd toxicity thresholds and underlying toxic modes of action (MOA) in aquatic biota (Herrmann et al., 2016; Malhotra et al., 2020). One of the best described MOA of Gd and other REY, is their interference with cellular/cross membrane calcium transport, which is key to a broad number of developmental and physiological processes across species (Ene et al., 2015). Conversely to the traditional perception, recent research has shown that some GBCAs and ionic Gd can accumulate in the vertebrate brain subsequent to administration, as seen in rats, pigs and humans (Choi and Moon, 2019; Kanda et al., 2016). In humans, administration of some GBCAs has been linked to neurotoxic responses (e.g. Lauer et al., 2021) as well as to a pathological condition termed 'nephrogenic systemic fibrosis" (Persson and Tepel, 2006). Many of the described adverse effects are related to de-chelation of the Gd ion from its chelating agent (Morcos, 2007; Perazella, 2007). For aquatic vertebrates, which are expectably at growing risk of exposure to anthropogenically derived Gd, toxicological testing and understanding are still fragmentary. To our knowledge, especially neurotoxic responses have not been comprehensively understood and described in aquatic organisms.

The aim of the present study is to deepen the understanding of Gd toxicity in aquatic vertebrates, with emphasis on effects on brain activity. We investigated and compared the ecotoxicological effects of Gd in form of an inorganic salt to a widely used macrocyclic GBCA on early life stages of zebrafish (*Danio rerio*). Acute toxicity (hatching success and survival), developmental parameters, brain activity and behavioural responses were studied.

2. Material and methods

2.1. Exposure solutions and validation

The Gd-based compounds tested in this study were the inorganic salt Gd(III) chloride hexahydrate ($GdCl_3$*$6H_2O$ powder, grade 99%, Sigma-Aldrich, CAS nr. 13450–84–5, Burlington, Massachusetts, USA) (hereafter $GdCl_3$) and Gadoterate meglumine (hereafter GBCA), a Gd-based contrast agent chelated with the ionic, macrocyclic molecule DOTA (2,2′,2″,2‴-(1,4,7,10-Tetraazacyclododecane-1,4,7,10-tetrayl)tetra-acetic acid), obtained as a pharmaceutically-ready injection solution. Exposures to (Gd-free) DOTA (TCI Europe, CAS nr. 60239–18–1, Zwijndrecht; Belgium) were included as background control. 3,4 dichloroaniline (3,4-DCA powder, purity >98%, Sigma-Aldrich, CAS 95-76-1, Burlington, Massachusetts, USA) was used as positive control.

Exposure solutions were prepared by either dissolving ($GdCl_3$, 3,4-DCA) or diluting (GBCA and DOTA) the different compounds in the zebrafish exposure medium, which was obtained from the zebrafish culture tanks and filtered through a 0.2 μm sterile vacuum filtration system (Nalgene®, Sigma-Aldrich) before use. Stock solutions were prepared at a nominal concentration of 3000 μg Gd L^{-1}, which were simultaneously the highest exposures (C1). The other exposure solutions were prepared by sequentially diluting the stock solution to nominal concentrations of 300 μg L^{-1} (C2), 30 μg L^{-1} (C3), 3 μg L^{-1} (C4) of Gd. DOTA was tested at the corresponding content in GBCA-C1 (7740 μg L^{-1}) and 3,4-DCA was tested at 4000 μg L^{-1}. Zebrafish exposure medium was used as negative control (Ctrl). The lower nominal exposure concentrations of Gd (C3 and C4) were selected to represent hospital wastewater discharges, where Gd was found to be from approximately 9 μg L^{-1} up to 55 μg L^{-1} ((Kümmerer and Helmers, 2000; Lerat-Hardy et al., 2019).

To validate exposure concentrations, samples were taken from the exposure containers at the end of the experiment. To obtain sufficient sample volumes, samples from all replicates had to be pooled. The samples (approximately 10 mL) were filtered (0.45 μm; Polyethersulfone syringe filter, AVANTOR, Radnor, Pennsylvania, USA), acidified with ultrapure HNO3 and kept at 4 °C until analyses with inductively coupled plasma-mass spectrometry (ICP-MS). Subsequently, the samples were diluted in 5% HNO3 and Gd concentrations analysed with an Agilent 8800 Triple Quadropole ICP-MS (Agilent, Santa Clara, California, USA) with SPS 4 Autosampler. Samples were quantified against standards from Inorganic Ventures with 115In as internal standard.

2.2. Zebrafish eggs

Fertilized eggs of the transparent zebrafish line *mitfa*$^{-/-}$ which lack melanophores (Lister J A et al., 1999) were obtained from the zebrafish facility at the Department of Biology (NTNU, Trondheim, Norway). Adult zebrafish were kept in 3.5 L tanks in a recirculating fish housing system (Techniplast; 28.0 ± 1.0 °C, pH 7 and 600 ppm osmolarity) under a dark-light cycle of 12:12 h. Fertilized eggs were obtained by crossing 2–3 females and 2–3 males in a breeding inlet. Eggs were rinsed

in fish water (FW; NaCl 0.2 g/L in carbon filtrated water) the following morning and transported to the laboratory in charge of conducting the exposure experiment (SINTEF Sealab, Trondheim, Norway) in thermally isolated polystyrene boxes.

2.3. Experimental set-up and daily monitoring

The toxicity assessment protocol applied in our study was adapted from the OECD Test No. 236: Fish Embryo Acute Toxicity (FET, OECD TG236) using zebrafish (*Danio rerio*) as test species (OECD, 2013). At approx. 6 h post-fertilization (hpf) 18–22 zebrafish eggs were transferred to 6-well plates (Ø = 3.5 cm COSTAR®) containing 10 mL of the respective Gd exposure medium (n = 4), 3,4-DCA as positive Ctrl (n = 4) or zebrafish exposure medium as control treatment (Ctrl,n = 6). The exposure duration was approximately 96 h. During all the experiment the temperature was kept at 28 °C and exposure solutions were renewed every 48 h. All the plastic equipment used during all the experimental steps was metal-free and previously acid-washed with 1 M HNO_3 (diluted with ultrapure water from 65% HNO_3 analysis grade, Sigma-Aldrich) and ultrapure water (MilliQ).

2.4. Hatching and survival

Hatched individuals were counted daily, and hatching success was assessed as the percentage of hatched individuals until the last day of exposure in relation to the initial number of embryos added at the start of the experiment. Mortality was evaluated throughout the experiment by counting and removing coagulated individuals (both embryos and larvae) from each well. At the end of the exposure period, no unhatched live embryos were found. Therefore, data will be presented (see section 3.1) as hatching success (which also accounts for the dead embryos throughout the experiment) and larvae survival.

2.5. Morphometry

Morphometrical measurements were performed using images of larvae (n = 5–8; approximately 120 hpf) selected randomly from each replicated exposure treatment, except for the positive control (3,4-DCA) where all the larvae had died by the end of the exposure period and before imaging. Images were taken of larvae embedded in methylcellulose, using a microscope (Eclipse 80i, Nikon Inc., Tokyo, Japan) equipped with Nikon PlanApo objectives (4x and 10x) and a Leica camera (MC170 HD, Wetzlar, Germany). Morphometric parameters, including eye area, eye minimum/maximum diameter, eye to front distance, body area, myotome length and myotome height, were automatically extracted from the microscope images using AutoMOMI, an automated software for morphometric measurements of fish larvae (Kvæstad et al., 2022).

2.6. Behaviour

Five larvae from each replicated treatment were placed in new well plates, and the well plates placed on a LED Backlight (Advanced Illumination, BX Series, 5x5in, White) for bright field imaging. The larvae were recorded for 10 min at 50 FPS using a Grashopper2 USB3 camera (FLIR, GS3-U3-51S5M − C, 5 MP, Monochrome) with a fixed focal lens (Edmund Optics, 67714, 16 mm, Barrington, New Jersey, USA) placed approximately 20 cm above the well plates, filming four wells at a time. The camera image data was encoded to MP4 video-files in real-time using a Jetson Nano running a custom software written in C++ and GStreamer. The larvae were detected and tracked via post-processing using an algorithm written Python 3.6 with OpenCV 4.4 software library Using the recorded swimming patterns, the average per larvae swimming distance, accumulated idle time and number of jumps where calculated and used as behavioural endpoints. The "idle time" starts to accumulate for each larva when it moves slower than 2 mm s^{-1} for 2 s or longer. The "number of jumps"-counter was incremented for each larva when swimming speed of more than 50 mm s^{-1} was measured.

2.7. Whole brain activity measurement using pERK/tERK mapping

Immunohistochemical detection and whole brain tri-dimensional maps of phosphorylated extracellular signal–regulated kinase (pERK) levels were performed according to the published *MAP-mapping* method (Randlett et al., 2015). Larvae from exposure concentrations C1 and C2, as well as Ctrl were sampled for neuronal analyses. Animals from the same treatment replicate were pooled in cell culture strainers in fresh zebrafish exposure medium, left to habituate for 45 min at room temperature, cold-euthanized and fixed overnight at 4 °C in fixative (0.25% Triton X-100 in 10% neutral buffered formalin solution, Sigma-Aldrich, Burlington, Massachusetts, USA). Larvae were labelled with primary antibodies pERK and tERK (Cell Signalling; Danvers, Massachusetts, USA, 1:600; 3 days at 4 °C) followed by secondary antibodies (Life technologies; Carlsbad, California, USA, 1/600; overnight at 4 °C). The larvae were mounted dorsal side-up in 2% low-melting point agarose (Sigma-Aldrich) and scanned using an upright confocal microscope (Zeiss 700) with a 10x/0.45 W water immersion objective at a resolution of 0.52× 0.52 × 2 μm/pixel. Two scans were taken for each fish to cover the whole brain and stitched together using the Pairwise Stitching Plugin in Fiji (Schindelin et al., 2009). Individual scans were first registered to the tERK reference brain from the Z-brain atlas using CMTK (Rohlfing and Maurer, 2003). The whole brain pERK maps were created by down sampling the scans to x = 300, y = 679 and z = 80 pixels, followed by smoothing with a 2D Gaussian blur filter.

2.8. Statistical analyses

Since hatching, larvae survival, morphometric and behavioural data did not meet the requirements for parametric statistics (normality and homogeneity tested with Shapiro−Wilk and Bartlett's tests respectively), comparisons between treatments were performed with Kruskal-Wallis test, followed by Dunn's pairwise post-hoc tests to identify groups that significantly differed from each other. Statistical significance was set at p-value <0.05 for all the analyses. All the statistical analyses were performed with R studio (v. 0.99.903, R core Team, 2016). Data are reported in text as mean ± standard error (SE).

For the whole brain activity measurement using pERK/tERK mapping, tri-dimensional pERK maps were compared across treatments with a Mann-Whitney *U* test corrected for false discovery-rate as described in Randlett et al. (2015).

3. Results

3.1. Gd exposure concentrations

The Gd concentrations measured in exposure solutions were within the expected nominal concentration ranges, beside $GdCl_3$ in exposure group C1, which was slightly lower (Table 1). Gd concentrations in Ctrl and DOTA exposures were 0.07–0.1 μg L^{-1} and 0.3 μg L^{-1} respectively.

3.2. Hatching success and larvae survival

Hatching success was not significantly different between exposure

Table 1
Gd exposure concentrations (μg L^{-1}) analysed in exposure solutions. Analysed samples were pooled replicates.

Dissolved Gd (μg L^{-1}) in exposure groups	C4	C3	C2	C1
Nominal	*3*	*30*	*300*	*3000*
Measured in $GdCl_3$	*4.9*	*31*	*307*	*2055*
Measured in GBCA	*3.4*	*32*	*295*	*3032*

groups, with an average hatching success of 91.4 ± 2.2% in the Ctrl group, and hatching being lowest in GBCA-C2, $GdCl_3$-C2 and DOTA with 89.4 ± 3.2, 88.9 ± 4.3 and 87.1 ± 5.3%, respectively (Fig. 1a). In the positive control groups (3,4-DCA) hatching success was 72.1 ± 2.7%, significantly lower compared to all other treatment groups including the Ctrl (p-values<0.05).

Similarly, survival of larvae was not significantly different between the exposure and Ctrl groups (p-value = 0.1). Survival ranged between 100% in the Ctrl group to 94.5 ± 3.4% in GBCA-C4 treatment group, following no clear concentration-dependent trends (Fig. 1b). In the positive Ctrl (3,4-DCA), all individuals died before the end of the experiment (120 h).

3.3. Larvae morphometry

Eye area, eye minimum/maximum diameter, eye to front distance, body area, myotome length and myotome height were analysed as morphometric endpoints in larvae. There were no significant differences between differently exposed larvae for any of the investigated morphometric endpoints (Table 2). Larvae eye to front distance showed variability between different treatment groups, ranging from 0.008 ± 0.003 mm in larvae of the DOTA exposed group to 0.016 ± 0.0002 and 0.016 ± 0.003 mm in GBCA-C4 and -C3. These differences were, however, not concentration dependent and neither i.e. significantly different between treatment groups (p-values = 0.5).

3.4. Effects on neural activity

Whole brain activity, assessed by pERK levels, was compared between larvae exposed to the two highest concentrations of $GdCl_3$ and the GBCA (C1 and C2) and larvae in the Ctrl group. Fig. 2 displays significant changes in brain activity, with decreased activities shown in magenta, and increased activities in green. Exposure to $GdCl_3$-C2 caused a decrease in brain activity compared to the Ctrl group, which was mostly restricted to the telencephalon (Fig. 2a, c). The neural activity in zebrafish exposed to $GdCl_3$-C1 also decreased compared to Ctrl (Fig. 2b). All major brain subdivisions were significantly affected, with the most substantial decreases in activity found in the telencephalon and rhombencephalon (Fig. 2c). In addition, larvae that were exposed to $GdCl_3$-C1 showed an increased pERK activity in the olfactory epithelium (Fig. 2b; green).

Conversely, the GBCA significantly increased activity in a few brain regions compared to the Ctrl (Fig. 2 d,e,f). GBCA-C2 caused increased activity mostly in the telencephalon, and in a small set of regions in the medulla and in the olfactory epithelium (Fig. 2 a,c). GBCA-C1 also produced a localized increase in activity, specifically in the olfactory epithelium, telencephalon, and a small part of the mesencephalon (Fig. 2 e,f).

3.5. Behaviour

Larval behavioural endpoints analysed in this study were swimming distance, number of jumps and idle time. No significant treatment- or concentration-dependent differences were found for these behavioural endpoints (Fig. 3 a,b,c).

4. Discussion

In this study, we determined the acute toxicity and sublethal effects of two forms of Gd, the inorganic salt $GdCl_3$ and a Gd containing

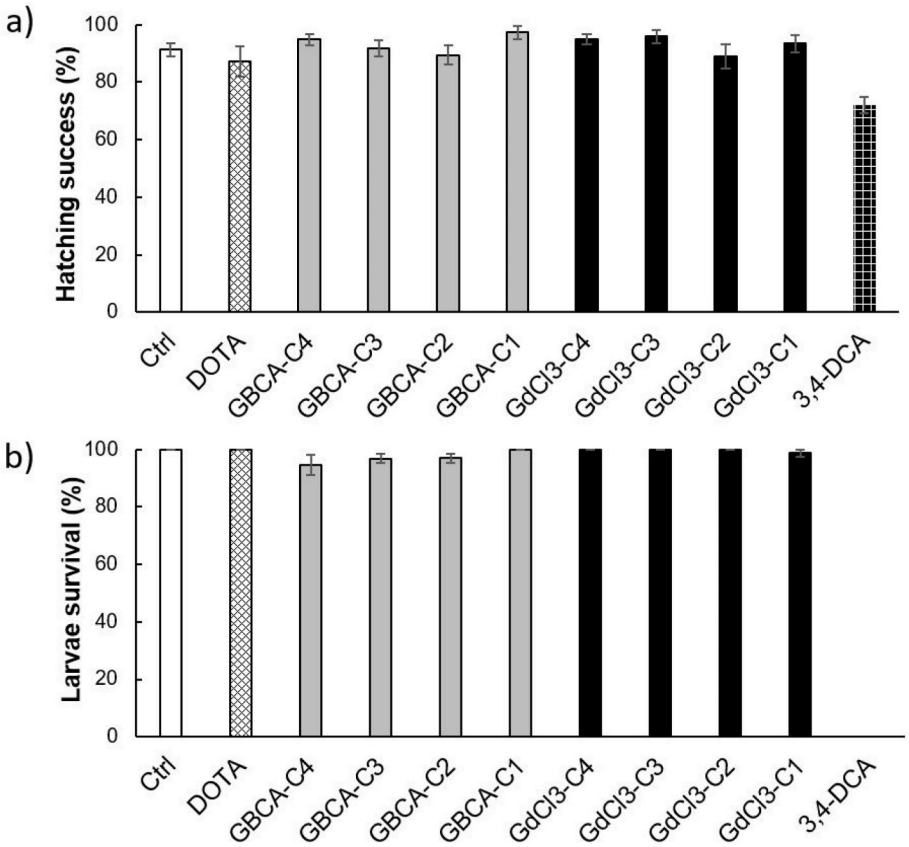

Fig. 1. Effects of Gd exposure (GBCA and $GdCl_3$) on (a) hatching success (% hatched individuals from total embryos), and (b) larvae survival (% of alive larvae at the end of the experiment of hatched individuals). in early life stages of zebrafish. Data are shown as percent survival (%) of total individuals, with columns representing the average (±SE) (n = 6 for Ctrl, n = 4 for all the other exposure groups).

Table 2
Morphometric data of zebrafish larvae (120 dpf) exposed to different concentrations of GdCl3 or GBCA. Data derive from five individuals of each replicate (n = 4) and are shown as mean ± SE.

Treatment	Eye area (mm^2)	Eye min diameter (mm)	Eye max diameter (mm)	Eye to front distance (mm)	Body area (mm^2)	Myotome length (mm)	Myotome height (mm)
Ctrl	0.08 ± 0.002	0.28 ± 0.003	0.35 ± 0.005	0.02 ± 0.002	1.15 ± 0.02	3.88 ± 0.02	0.30 ± 0.006
DOTA	0.07 ± 0.002	0.28 ± 0.006	0.34 ± 0.004	0.01 ± 0.004	1.21 ± 0.01	3.93 ± 0.02	0.31 ± 0.004
GBCA-C4	0.08 ± 0.001	0.28 ± 0.002	0.35 ± 0.003	0.02 ± 0.003	1.18 ± 0.02	3.85 ± 0.04	0.31 ± 0.005
GBCA-C3	0.08 ± 0.001	0.28 ± 0.003	0.35 ± 0.003	0.02 ± 0.002	1.17 ± 0.02	3.84 ± 0.03	0.31 ± 0.006
GBCA-C2	0.07 ± 0.002	0.28 ± 0.004	0.34 ± 0.005	0.02 ± 0.001	1.16 ± 0.02	3.87 ± 0.05	0.30 ± 0.003
GBCA-C1	0.07 ± 0.002	0.28 ± 0.005	0.34 ± 0.004	0.01 ± 0.004	1.17 ± 0.02	3.86 ± 0.03	0.31 ± 0.003
GdCl3-C4	0.07 ± 0.002	0.28 ± 0.005	0.34 ± 0.006	0.01 ± 0.002	1.17 ± 0.01	3.83 ± 0.03	0.31 ± 0.002
GdCl3-C3	0.08 ± 0.003	0.28 ± 0.004	0.34 ± 0.006	0.02 ± 0.003	1.18 ± 0.01	3.87 ± 0.03	0.31 ± 0.004
GdCl3-C2	0.07 ± 0.003	0.27 ± 0.006	0.34 ± 0.008	0.01 ± 0.000	1.19 ± 0.01	3.85 ± 0.05	0.31 ± 0.006
GdCl3-C1	0.07 ± 0.003	0.27 ± 0.007	0.34 ± 0.003	0.01 ± 0.004	1.17 ± 0.01	3.80 ± 0.03	0.32 ± 0.01

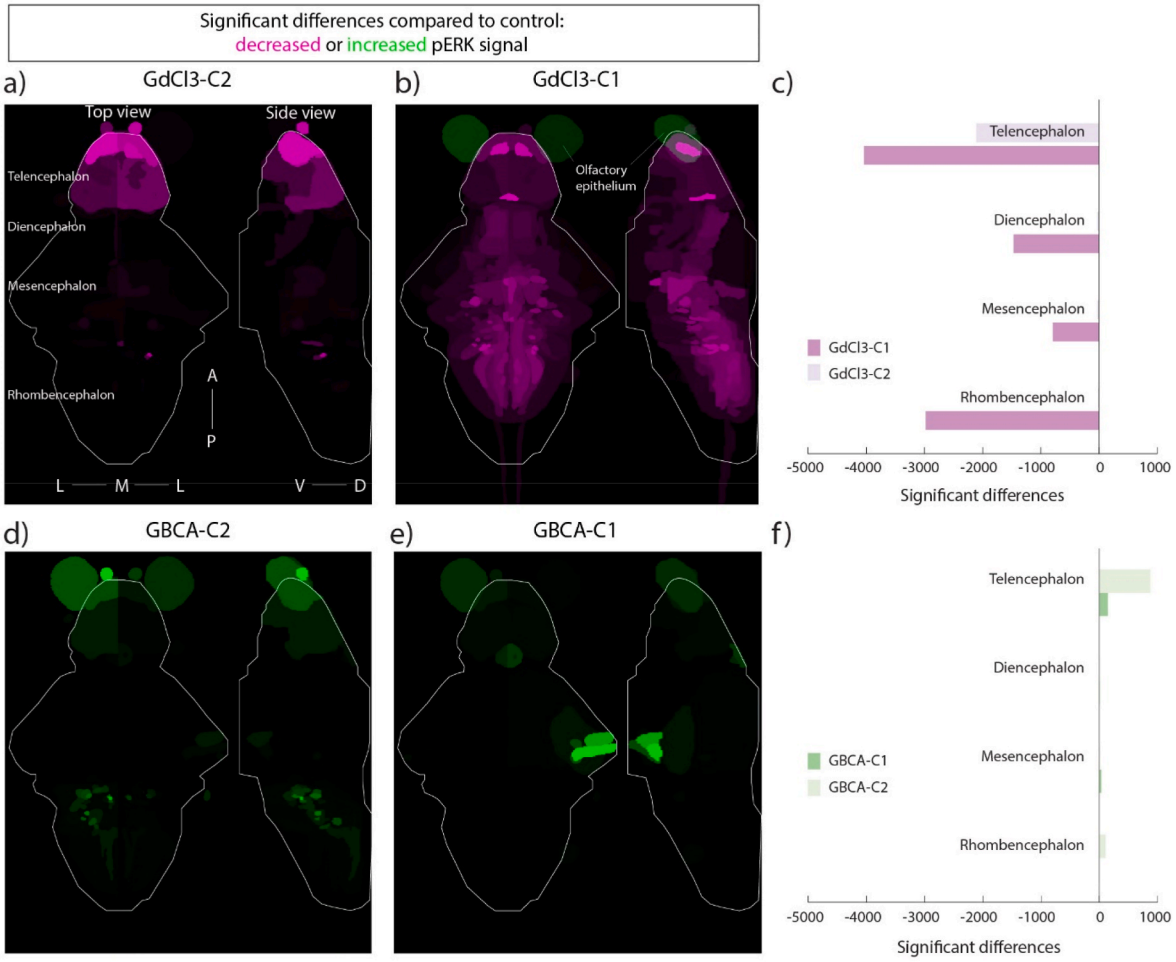

Fig. 2. Whole brain significant differences in pERK levels after exposure to $GdCl_3$ and GCBA. Maps of significant differences in pERK levels in larvae exposed to **a)** $GdCl_3$-C2 ($n = 17$), **b)** $GdCl_3$ -C1 ($n = 14$), **d)** GBCA-C2 ($n = 13$), **e)** GBCA-C1 ($n = 18$) *vs* Ctrl (n = 19 and 16 for comparison with $GdCl_3$ and GBCA, respectively). Quantification of significant differences in pERK levels in major brain subdivisions in zebrafish larvae exposed to **c)** $GdCl_3$-C2 and $GdCl_3$ -C1 and **f)** GBCA-C2 and -C1 compared to Ctrl larvae.

macrocyclic medical contrast agent here referred to as GBCA, on early life stages of zebrafish. Our results show that the tested Gd concentrations (up to 3032 μg L^{-1} measured concentration) were not acutely toxic to zebrafish embryos and larvae, neither as the inorganic salt $GdCl_3$, nor as contrast agent. Similarly, we found no effects on development, growth (body area, length) or malformation rate. This agrees with previous findings on toxicity of inorganic Gd compounds in zebrafish early life-stages. Zhao et al. (2021) derived a median lethal concentration (LC_{50}) of 7800 μg L^{-1}, while Romero-Freire et al. (2019) found no mortality in developing zebrafish for up to 5000 μg L^{-1} $GdCl_3$ after a 96-h exposure. The latter study, however, reported a substantial decrease in Gd concentration in the exposure medium over time due to precipitation of the $GdCl_3$ salt promoted by carbonate or sulphate groups in the media. These findings agree with those of our study, where the measured Gd concentration was slightly lower than the nominal concentration in the high $GdCl_3$ exposure groups (C1; nominal 3000 μg L^{-1} vs measured 2055 μg L^{-1}), suggesting oversaturation and limited solubility of Gd in the testing media. We observed a similar effect at equal

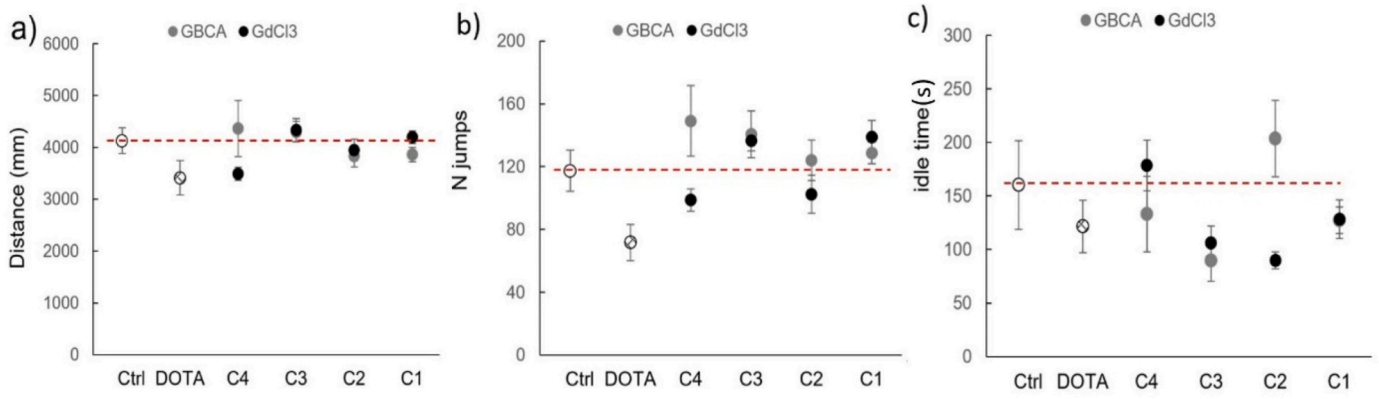

Fig. 3. Behavioural parameters **a)** average distance swam by each larva (mm) during the total recording time of 10 min; **b)** number of jumps (>50 mm s^{-1}); and **c)** idle time (>2 s) expressed in seconds, as measured on 5 larvae for each replicate (n = 6 for Ctrl and n = 4 replicated well for all the other exposures). Data are expressed as mean ± SE. The red line marks average Ctrl values along the y axes for better visualisation.

nominal concentrations in a seawater experiment (Farkas et al. in preparation). This indicates that solubility limits of Gd- (and other REY-) salts need to be considered and the correspondence between nominal concentrations and actual concentrations should always be validated in exposure studies.

While we found no significant effects on mortality or development in this study, we observed that different Gd compounds affected the brain activity differently. Our results showing a globally decrease in brain activity after exposure to unchelated Gd are in line with prior works reporting Gd^{3+}-induced inhibition of ion channels that regulate the excitability of neurons. Unchelated Gd^{3+} was reported to inhibit stretch-activated cation channels and voltage-gated calcium channels (Bourne and Trifaró, 1982; Ermakov et al., 2010; Yang and Sachs, 1989). In contrast to $GdCl_3$ exposure, the chelated Gd^{3+} (GBCA) did not produce an activity suppression, but instead resulted in a minor and localised activity increase at the highest concentrations. This suggests that the macrocyclic GBCA was stable under the present study conditions and that there was no (or limited) exposure of the neural tissue to de-chelated Gd^{3+},

A common feature observed in larvae post-exposure to $GdCl_3$ (C1) and GBCA (C1 and C2) was an increased pERK level in the olfactory epithelium. The mechanism mediating the increase in pERK in the epithelium, as opposed to the broad neuronal inhibition observed $GdCl_3$-exposed larvae, is unclear. The olfactory epithelium is in direct contact with the aquatic environment and is, therefore, potentially more exposed to dissolved REY. Interestingly, oxidative stress has been shown to induce ERK phosphorylation and cell death in retinal pigment epithelial cells (Garg and Chang, 2003). Therefore, elevated pERK levels in the olfactory region might be a result of Gd-induced oxidative stress and neurodegeneration.

The potent $GdCl_3$-induced inhibition of activity in regions of the teleost brain supporting locomotion (Carbo-Tano et al., 2023), learning and memory (Lal et al., 2018) and odour-driven foraging and reproduction (Kermen et al., 2013) indicates that exposure to unchelated Gd^{3+} has the potential to alter these behaviours which are crucial for long-term survival.

The fact that we did not detect a clear trend in altered locomotion in $GdCl_3$ exposed larvae suggests that the measurement of neural activity using pERK might be more sensitive to subtle physiological changes than the assessment of locomotion using behavioural assays. Since learning and memory as well as reproductive behaviours are fully developed and expressed weeks after the larval stage used in this experiment (Palumbo et al., 2020), it would be relevant to assess the long-term behavioural effects of early-life $GdCl_3$ exposure, for example at the juvenile and adult stages.

The lack of locomotive behavioural responses in this study can also be attributed to methodological limitations. Particularly, to ensure the fish well-being during the imaging and to avoid significant differences in the exposure time between the first and last imaged group, the filming time used in this study was reduced to 10 min compared to previous tests with other species where the recording time was set at 20 min. This was done because pilot experiments showed that in the imaging set-up (with strong lights causing increasing temperature) larvae appeared to suffer reduced oxygen levels in the exposure media when assessed for more than 10 min.

Overall, our study highlights the importance of studying well-selected sublethal endpoints that are adapted to the (expected) MOA of the test compound(s). The fish embryo toxicity test (OECD, 2013) has become a standard component for environmental risk assessment of chemicals. While one of the major advantages of standardising ecotoxicological test organisms and study endpoints is high comparability across studies and chemicals, there is a clear limitation in transferability of toxicity thresholds to other fish species, environmental compartments, and geographic areas (Hansen et al., 2021). While MOA of a chemical compound may be more easily identified in a well-studied model species, the use of standard endpoints only can also miss more subtle responses and/or more specific effect mechanism, as demonstrated in the present study. Indeed, the use of only standard endpoints would have failed to unveil $GdCl_3$ and GBCA-induced changes in the brain activity of the zebrafish larvae, therefore, neglecting key information relevant for environmental risk assessment of Gd-based compounds and preventing further investigation of related biological implications.

5. Conclusion

This study investigating the acute toxicity and sublethal effects of two forms of Gd (inorganic salt $GdCl_3$ and as macrocyclic GBCA) on early life stages of zebrafish demonstrates that the two tested compounds were not acutely toxic to zebrafish embryos and larvae after 96 h of exposure. Similarly, we did not find effects on development. While no changes were observed in locomotive behaviour, we found distinct alterations in the brain activity of larvae exposed to the highest concentrations of $GdCl_3$ and the GBCA. These findings show that free Gd may have previously unnoticed effects on developing fish, highlighting the necessity of investigating the long-term fate and effects of the most used GBCAs released into the environment. This study further shows the importance of also including targeted non-standard endpoints for effective ecotoxicological risk estimation.

Funding

This work was supported by the Norwegian Research Council under the project ELEMENTARY (Grant agreement NO. 301236) and by the funding scheme for independent projects (FRIPRO) to F.K. (Grant agreement NO. 262698).

CRediT authorship contribution statement

Stefania Piarulli: Writing - review & editing, Writing - original draft, Visualization, Investigation, Formal analysis, Data curation, Conceptualization. **Juliane A. Riedel:** Writing - review & editing, Writing - original draft, Visualization, Investigation, Formal analysis, Data curation, Conceptualization. **Frida N. Fossum:** Visualization, Investigation, Formal analysis, Data curation. **Florence Kermen:** Writing - review & editing, Writing - original draft, Visualization, Supervision, Resources, Methodology, Investigation, Funding acquisition, Formal analysis, Data curation. **Bjørn Henrik Hansen:** Writing - review & editing, Validation, Methodology, Investigation, Formal analysis, Conceptualization. **Bjarne Kvæstad:** Writing - review & editing, Writing - original draft, Methodology, Investigation, Formal analysis, Data curation. **Pål A. Olsvik:** Writing - review & editing, Supervision, Resources. **Julia Farkas:** Writing - review & editing, Writing - original draft, Validation, Supervision, Resources, Methodology, Investigation, Funding acquisition, Formal analysis, Conceptualization.

Declaration of competing interest

The authors declare that they have no known competing financial interests or personal relationships that could have appeared to influence the work reported in this paper.

Data availability

Data will be made available on request.

References

Bau, M., Dulski, P., 1996. Anthropogenic origin of positive gadolinium anomalies in river waters. Earth Planet Sci. Lett. 143, 245–255. https://doi.org/10.1016/0012-821x(96)00127-6.

Bourne, G.W., Trifaró, J.M., 1982. The gadolinium ion: a potent blocker of calcium channels and catecholamine release from cultured chromaffin cells. Neuroscience 7, 1615–1622. https://doi.org/10.1016/0306-4522(82)90019-7.

Brünjes, R., Hofmann, T., 2020. Anthropogenic gadolinium in freshwater and drinking water systems. Water Res. 182, 115966 https://doi.org/10.1016/j.watres.2020.115966.

Caravan, P., Ellison, J.J., McMurry, T.J., Lauffer, R.B., 1999. Gadolinium(III) chelates as MRI contrast agents: structure, dynamics, and applications. Chem. Rev. 99, 2293–2352. https://doi.org/10.1021/cr980440x.

Carbo-Tano, M., Lapoix, M., Jia, X., Thouvenin, O., Pascucci, M., Auclair, F., Quan, F.B., Albadri, S., Aguda, V., Farouj, Y., C Hillman, E.M., Portugues, R., Del Bene, F., Thiele, T.R., Dubuc, R., Wyart, C., 2023. The mesencephalic locomotor region recruits distributed V2a reticulospinal neurons to drive forward locomotion. Nat. Neurosci. 26, 1775–1790.

Choi, J.W., Moon, W., 2019. Gadolinium deposition in the brain and body. J. Belgian Soc. Radiol. 103, 134–147. https://doi.org/10.5334/jbsr.1945.

Ene, C.D., Ruta, L.L., Nicolau, I., Popa, C.V., Iordache, V., Neagoe, A.D., Farcasanu, I.C., 2015. Interaction between lanthanide ions and Saccharomyces cerevisiae cells. J. Biol. Inorg. Chem. 20, 1097–1107. https://doi.org/10.1007/s00775-015-1291-1.

Ermakov, Y.A., Kamaraju, K., Sengupta, K., Sukharev, S., 2010. Gadolinium ions block mechanosensitive channels by altering the packing and lateral pressure of anionic lipids. Biophys. J. 98, 1018–1027. https://doi.org/10.1016/j.bpj.2009.11.04.

Garg, T.K., Chang, J.Y., 2003. Oxidative stress causes ERK phosphorylation and cell death in cultured retinal pigment epithelium: prevention of cell death by AG126 and 15-deoxy-delta 12, 14-PGJ2. BMC Ophthalmol. 3, 1–15. https://doi.org/10.1186/1471-2415-3-5.

Gwenzi, W., Mangori, L., Danha, C., Chaukura, N., Dunjana, N., Sanganyado, E., 2018. Sources, behaviour, and environmental and human health risks of high-technology rare earth elements as emerging contaminants. Sci. Total Environ. 636, 299–313. https://doi.org/10.1016/j.scitotenv.2018.04.235.

Hansen, B.H., Farkas, J., Piarulli, S., Vicario, S., Kvæstad, B., Williamson, D.R., Sørensen, L., Davies, E.J., Nordtug, T., 2021. Atlantic cod (*Gadus morhua*) embryos are highly sensitive to short-term 3,4-dichloroaniline exposure. Toxicol Rep 8, 1754–1761. https://doi.org/10.1016/j.toxrep.2021.10.006.

Hatje, V., Bruland, K.W., Flegal, A.R., 2016. Increases in anthropogenic gadolinium anomalies and rare earth element concentrations in San Francisco bay over a 20 Year record. Environ. Sci. Technol. 50, 4159–4168. https://doi.org/10.1021/acs.est.5b04322.

Herrmann, H., Nolde, J., Berger, S., Heise, S., 2016. Aquatic ecotoxicity of lanthanum - a review and an attempt to derive water and sediment quality criteria. Ecotoxicol. Environ. Saf. 124, 213–238. https://doi.org/10.1016/j.ecoenv.2015.09.033.

Kamenopoulos, S.N., Shields, D., Agioutantis, Z., 2015. Sustainable Development Criteria and Indicators for the Assessment of Rare Earth Element Mining Projects, Rare Earths Industry: Technological, Economic, and Environmental Implications. Elsevier Inc. https://doi.org/10.1016/B978-0-12-802328-0.00006-1.

Kanda, T., Oba, H., Toyoda, K., Kitajima, K., Furui, S., 2016. Brain gadolinium deposition after administration of gadolinium-based contrast agents. Jpn. J. Radiol. 34, 3–9. https://doi.org/10.1007/s11604-015-0503-5.

Kermen, F., Franco, L.M., Wyatt, C., Yaksi, E., 2013. Neural circuits mediating olfactory-driven behavior in fish. Front. Neural Circ. 7, 1–9. https://doi.org/10.3389/fncir.2013.00062.

Knappe, A., Möller, P., Dulski, P., Pekdeger, A., 2005. Positive gadolinium anomaly in surface water and ground water of the urban area Berlin, Germany. Chemie der Erde 65, 167–189. https://doi.org/10.1016/j.chemer.2004.08.004.

Kümmerer, K., Helmers, E., 2000. Hospital effluents as a source of gadolinium in the aquatic environment. Environ. Sci. Technol. 34, 573–577. https://doi.org/10.1021/es990633h.

Kvæstad, B., Hansen, B.H., Davies, E., 2022. Automated morphometrics on microscopy images of Atlantic cod larvae using Mask R-CNN and classical machine vision techniques. MethodsX 9. https://doi.org/10.1016/j.mex.2021.101598.

Lal, P., Tanabe, H., Suster, M.L., Ailani, D., Kotani, Y., Muto, A., Itoh, M., Iwasaki, M., Wada, H., Yaksi, E., Kawakami, K., 2018. Identification of a neuronal population in the telencephalon essential for fear conditioning in zebrafish. BMC Biol. 16, 1–18. https://doi.org/10.1186/s12915-018-0502-y.

Lauer, M., Lauer, A., You, S.J., Kluge, S., Hattingen, E., Harter, P.N., Senft, C., Wagner, M., Voss, M., 2021. Neurotoxicity of subarachnoid Gd-based contrast agent accumulation: a potential complication of intraoperative MRI? Neurosurg. Focus 50. https://doi.org/10.3171/2020.10.FOCUS20402.

Lerat-Hardy, A., Coynel, A., Dutruch, L., Pereto, C., Bossy, C., Gil-Diaz, T., Capdeville, M. J., Blanc, G., Schäfer, J., 2019. Rare earth element fluxes over 15 years into a major European estuary (Garonne-Gironde, SW France): hospital effluents as a source of increasing gadolinium anomalies. Sci. Total Environ. 656, 409–420. https://doi.org/10.1016/j.scitotenv.2018.11.343.

Lister, J A, Robertson, C P, Lepage, T, Johnson, S L, Raible, D W, 1999. Nacre Encodes a Zebrafish Microphthalmia-Related Protein That Regulates Neural-Crest-Derived Pigment Cell Fate. Development 126, 3757–3767.

Malhotra, N., Hsu, H.S., Liang, S.T., Roldan, M.J.M., Lee, J.S., Ger, T.R., Hsiao, C. Der, 2020. An updated review of toxicity effect of the rare earth elements (REEs) on aquatic organisms. Animals 10, 1–27. https://doi.org/10.3390/ani10091663.

Merschel, G., Bau, M., Schmidt, K., Münker, C., Dantas, E.L., 2017. Hafnium and neodymium isotopes and REY distribution in the truly dissolved, nanoparticulate/colloidal and suspended loads of rivers in the Amazon Basin, Brazil. Geochim. Cosmochim. Acta 213, 383–399. https://doi.org/10.1016/j.gca.2017.07.006.

Morcos, S.K., 2007. Nephrogenic systemic fibrosis following the administration of extracellular gadolinium based contrast agents: is the stability of the contrast agent molecule an important factor in the pathogenesis of this condition? Br. J. Radiol. 80, 73–76. https://doi.org/10.1259/bjr/17111243.

Nozaki, Y., Lerche, D., Alibo, D.S., Tsutsumi, M., 2000. Dissolved indium and rare earth elements in three Japanese rivers and Tokyo Bay: evidence for anthropogenic Gd and in. Geochim. Cosmochim. Acta 64, 3975–3982. https://doi.org/10.1016/S0016-7037(00)00472-5.

OECD, 2013. Test No. 236: fish embryo acute toxicity (FET) test. OECD Guidel. Test. Chem. Sect. 2. OECD Publ, 1–22.

Palumbo, F., Serneels, B., Pelgrims, R., Yaksi, E., 2020. The zebrafish dorsolateral habenula is required for updating learned behaviors. Cell Rep. 32, 108054 https://doi.org/10.1016/j.celrep.2020.108054.

Parant, M., Perrat, E., Wagner, P., Rosin, C., Py, J.S., Cossu-Leguille, C., 2018. Variations of anthropogenic gadolinium in rivers close to waste water treatment plant discharges. Environ. Sci. Pollut. Res. 25, 36207–36222. https://doi.org/10.1007/s11356-018-3489-6.

Perazella, M.A., 2007. Nephrogenic systemic fibrosis, kidney disease, and gadolinium: is there a link? Clin. J. Am. Soc. Nephrol. 2, 200–202. https://doi.org/10.2215/CJN.00030107.

Persson, P.B., Tepel, M., 2006. Contrast medium-induced nephropathy: the pathophysiology. Kidney Int. 69, S8–S10. https://doi.org/10.1038/sj.ki.5000367.

Piarulli, S., Hansen, B.H., Ciesielski, T., Zocher, A.L., Malzahn, A., Olsvik, P.A., Sonne, C., Nordtug, T., Jenssen, B.M., Booth, A.M., Farkas, J., 2021. Sources, distribution and effects of rare earth elements in the marine environment: current knowledge and research gaps. Environ. Pollut. 291 https://doi.org/10.1016/j.envpol.2021.118230.

Port, M., Idée, J.M., Medina, C., Robic, C., Sabatou, M., Corot, C., 2008. Efficiency, thermodynamic and kinetic stability of marketed gadolinium chelates and their possible clinical consequences: a critical review. Biometals 21, 469–490. https://doi.org/10.1007/s10534-008-9135-x.

Randlett, O., Wee, C.L., Naumann, E.A., Nnaemeka, O., Schoppik, D., Fitzgerald, J.E., Portugues, R., Lacoste, A.M.B., Riegler, C., Engert, F., Schier, A.F., 2015. Whole-brain activity mapping onto a zebrafish brain atlas. Nat. Methods 12, 1039–1046. https://doi.org/10.1038/nmeth.3581.

Rohlfing, T., Maurer, C.R., 2003. Nonrigid image registration in shared-memory multiprocessor environments with application to brains, breasts, and bees. IEEE Trans. Inf. Technol. Biomed. 7, 16–25. https://doi.org/10.1109/TITB.2003.808506.

Romero-Freire, A., Joonas, E., Muna, M., Cossu-Leguille, C., Vignati, D.A.L., Giamberini, L., 2019. Assessment of the toxic effects of mixtures of three lanthanides (Ce, Gd, Lu) to aquatic biota. Sci. Total Environ. 661, 276–284. https://doi.org/10.1016/j.scitotenv.2019.01.155.

Runge, V.M., 2018. Dechelation (Transmetalation): consequences and safety concerns with the linear gadolinium-based contrast agents, in view of recent health care rulings by the EMA (Europe), FDA (United States), and PMDA (Japan). Invest. Radiol. 53, 571–578. https://doi.org/10.1097/RLI.0000000000000507.

Schindelin, J., Arganda-Carrera, I., Frise, E., Verena, K., Mark, L., Tobias, P., Stephan, P., Curtis, R., Stephan, S., Benjamin, S., Jean-Yves, T., Daniel, J.W., Volker, H., Kevin, E., Pavel, T., Albert, C., 2009. Fiji - an Open platform for biological image analysis. Nat. Methods 9. https://doi.org/10.1038/nmeth.2019.Fiji.

Wahsner, J., Gale, E.M., Rodríguez-Rodríguez, A., Caravan, P., 2019. Chemistry of MRI contrast agents: current challenges and new frontiers. Chem. Rev. 119, 957–1057. https://doi.org/10.1021/acs.chemrev.8b00363.

Yang, X.C., Sachs, F., 1989. Block of stretch-activated ion channels in xenopus oocytes by gadolinium and calcium ions. Science 243, 1068–1071. https://doi.org/10.1126/science.2466333.

Zhao, Y., Liang, J., Meng, H., Yin, Y., Zhen, H., Zheng, X., Shi, H., Wu, X., Zu, Y., Wang, B., Fan, L., Zhang, K., 2021. Rare earth elements lanthanum and praseodymium adversely affect neural and cardiovascular development in zebrafish (*Danio rerio*). Environ. Sci. Technol. 55, 1155–1166. https://doi.org/10.1021/acs.est.0c06632.